cancers

MDPI

Article

Cellular and Molecular Effects of Eribulin in Preclinical Models of Hematologic Neoplasms

Hugo Passos Vicari [1], Keli Lima [1,2], Leticia Veras Costa-Lotufo [1] and João Agostinho Machado-Neto [1,*]

[1] Department of Pharmacology, Institute of Biomedical Sciences, University of São Paulo, São Paulos 05508-000, Brazil
[2] Laboratory of Medical Investigation in Pathogenesis and Targeted Therapy in Onco-Immuno-Hematology (LIM-31), Department of Internal Medicine, Hematology Division, Faculdade de Medicina, University of São Paulo, São Paulo 01246-903, Brazil
* Correspondence: jamachadoneto@usp.br; Tel.: +55-11-3091-7467

Simple Summary: Hematologic neoplasms comprise a heterogeneous group of diseases that interfere with normal blood production. Treating patients who fail available therapies for these diseases is an ongoing challenge. Thus, the search for new treatment options is urgent, and drug repositioning is emerging as an attractive strategy for finding new effective drugs. Eribulin is a drug that acts on microtubules, and it is used in solid tumors, and its safety is known. In the present study, we provide evidence of the effects of eribulin on hematologic cancers and identify the potential biomarkers of responsiveness. Our study indicates that eribulin is a candidate blood cancer drug for repositioning.

Abstract: Despite the advances in understanding the biology of hematologic neoplasms which has resulted in the approval of new drugs, the therapeutic options are still scarce for relapsed/refractory patients. Eribulin is a unique microtubule inhibitor that is currently being used in the therapy for metastatic breast cancer and soft tissue tumors. Here, we uncover eribulin's cellular and molecular effects in a molecularly heterogeneous panel of hematologic neoplasms. Eribulin reduced cell viability and clonogenicity and promoted apoptosis and cell cycle arrest. The minimal effects of eribulin observed in the normal leukocytes suggested selectivity for malignant blood cells. In the molecular scenario, eribulin induces DNA damage and apoptosis markers. The *ABCB1*, *ABCC1*, p-AKT, p-NFκB, and NFκB levels were associated with responsiveness to eribulin in blood cancer cells, and a resistance eribulin-related target score was constructed. Combining eribulin with elacridar (a P-glycoprotein inhibitor), but not with PDTC (an NFkB inhibitor), increases eribulin-induced apoptosis in leukemia cells. In conclusion, our data indicate that eribulin leads to mitotic catastrophe and cell death in blood cancer cells. The expression and activation of MDR1, PI3K/AKT, and the NFκB-related targets may be biomarkers of the eribulin response, and the combined treatment of eribulin and elacridar may overcome drug resistance in these diseases.

Keywords: eribulin; microtubule dynamics; acute leukemias; drug resistance

Citation: Vicari, H.P.; Lima, K.; Costa-Lotufo, L.V.; Machado-Neto, J.A. Cellular and Molecular Effects of Eribulin in Preclinical Models of Hematologic Neoplasms. *Cancers* **2022**, *14*, 6080. https://doi.org/10.3390/cancers14246080

Academic Editors: Laura Bracci, Antonella Sistigu and Pierpaolo Correale

Received: 20 October 2022
Accepted: 6 December 2022
Published: 10 December 2022

1. Introduction

Hematologic neoplasms comprise a heterogeneous group of diseases that interfere with the normal production of blood cells, among which, acute leukemias stand out for their high mortality and recurrence rates [1]. Despite the great advances in understanding the biology of these diseases which has resulted in the approval of new drugs, the therapeutic options are still scarce for the relapsed/refractory patients [2,3].

Microtubules are essential components for cell division due to their contractile properties, and they are considered one of the most important molecular targets for cancer treatment. Microtubule-targeting agents suppress microtubule dynamics and present variation in terms of the modulation (stabilizing and destabilizing activity) and binding

sites to tubulin [4–6]. Indeed, antimicrotubule therapy has been widely used, and it has significantly contributed to cancer therapy over the past 50 years. The vinca alkaloids (vincristine, vinblastine, vindesine, vinorelbine, and vinflunine) represent the oldest class of microtubule-interfering agents, and they have been used to treat a wide range of malignancies, including leukemias, lymphomas, and solid tumors [7]. Paclitaxel and its semi-synthetic analog docetaxel have been utilized for treating advanced ovarian, breast, lung, head and neck, and prostate cancers [8].

In the context of hematologic malignancies, vinca alkaloids are extensively used in the treatment of acute lymphoblastic leukemia (ALL) [9], with vincristine being one of the few drugs that is approved for the treatment of relapsing T-ALL [10]. In addition, several tubulin inhibitors are in ongoing clinical trials against acute myeloid leukemia (AML) [11].

Despite the considerable number of microtubule-modulating agents available, the mechanisms that limit the effectiveness of the current treatments, such as the overexpression of specific tubulin isoforms, mutations, and other mechanisms of resistance which have not yet been elucidated, are a significant clinical problem, and this reinforces the need for the search for new and more selective agents that may act against resistant cells [12–14].

Recently, a unique microtubule inhibitor, eribulin, has drawn attention due to its anticancer properties. It is currently being used in metastatic breast cancer and soft tissue tumor therapy [15,16], but its effects on blood cancers have been underexplored. Here, we show that eribulin provides potent antineoplastic effects in a molecularly heterogeneous panel of blood cancer cells, and we uncover the underlying anticancer molecular mechanisms.

2. Materials and Methods

2.1. Healthy Donors' Samples

Peripheral blood mononuclear cells (PBMCs) were obtained from eight healthy donors by Ficoll-Hypaque density gradient centrifugation (Sigma-Aldrich, St. Louis, MO, USA) according to the manufacturer's instructions. All of the procedures were approved by the Ethics Committee of the Institute of Biomedical Sciences of the University of São Paulo (CAAE: 39510920.1.0000.5467). Informed consent was obtained from all of the donors, and all of the methods were conducted in accordance with the Declaration of Helsinki. The PBMCs were cultured in RPMI-1640 medium containing 30% fetal bovine serum (FBS), penicillin/streptomycin, and recombinant cytokines (30 ng/mL IL3, 100 ng/mL IL7, 100 ng/mL FLT3-ligand, and 30 ng/mL SCF, PeproTech, Rocky Hill, NJ, USA) at a density of 2×10^6 cells/mL.

2.2. Cell Culture and Chemical Reagents

The OCI-AML3, Kasumi-1, HL-60, THP-1, MOLM-13, MV4-11, NB4, and NB4-R2 cells were kindly provided by Prof. Eduardo Magalhães Rego (University of São Paulo, Ribeirão Preto, Brazil). The U-937, K-562, KU812, HEL, Jurkat, Namalwa, Daudi, Raji, U266, MM1.S, and MM1.R cells were kindly provided by Prof. Sara Teresinha Olalla Saad (University of Campinas, Campinas, Brazil). The CEM, NALM6, and REH were kindly provided by Dr. Gilberto Carlos Franchi Junior (University of Campinas, Campinas, Brazil). The SET-2 cells were kindly provided by Prof. Fabíola Attié de Castro (University of São Paulo, Ribeirão Preto, Brazil). Karpas 442 was kindly provided by Prof. Martin Dreyling (University Hospital Grosshadern/LMU, Munich, Germany). SUP-B15 was kindly provided by Dr. Lucas Eduardo Botelho de Souza (National Institute of Science and Technology in Stem Cells and Cell Therapy, Ribeirão Preto, São Paulo, Brazil).

The cells were cultured in an appropriate media (RPMI-1640, IMDM, or alpha-MEM) supplemented with 10 or 20% FBS according to the American Type Culture Collection (ATCC) or Deutsche Sammlung von Mikroorganismen und Zellkulturen (DSMZ) recommendations, plus 1% penicillin/streptomycin. The cell cultures were maintained at 5% CO_2 and 37 °C. Eribulin mesylate was purchased from Sigma-Aldrich.

2.3. Cell Viability Assay

A total of 2×10^4 cells (cell lines) or 2×10^5 (PBMC) per well were seeded in 96-well plates in the appropriate medium in the presence of a vehicle or different concentrations of eribulin (0, 0.032, 0.16, 0.8, 4, 20, or 100 nM for 72 h or 0, 0.062, 0.125, 0.25, 0.5, 1, or 2 nM for 24, 48, and 72 h). Next, 10 µL methylthiazoletetrazolium (MTT) solution (5 mg/mL) was added and incubated at 37 °C in 5% CO_2 for 4 h. The reaction was stopped with 150 µL 0.1 N HCl in anhydrous isopropanol. The cell viability was evaluated by measuring the absorbance at 570 nm. The IC_{50} values were calculated using nonlinear regression analysis in GraphPad Prism 5 (GraphPad Software, Inc., San Diego, CA, USA).

2.4. Apoptosis Assay

A total of 1×10^5 cells per well were seeded in 24-well plates in the presence of a vehicle or eribulin (0.25, 0.5, and 1 nM) for 72 h. The cells were then washed twice with ice-cold PBS and resuspended in a binding buffer containing 1 µg/mL propidium iodide (PI), and 1 µg/mL APC-labeled annexin V (BD Biosciences, San Jose, CA, USA). All of the specimens were acquired by flow cytometry (FACSCalibur; Becton Dickinson, Franklin Lakes, NJ, USA) after incubation for 15 min at room temperature in a light-protected area, and they were analyzed using FlowJo software (Treestar, Inc., San Carlos, CA, USA).

2.5. Cell Cycle Analysis

A total of 4×10^5 cells per well were seeded in six-well plates in the presence of a vehicle or eribulin (0.25, 0.5, and 1 nM), harvested at 72 h, fixed with 70% ethanol, and stored at 4 °C for at least 2 h before the analysis. The fixed cells were stained with 20 µg/mL PI containing 10 µg/mL RNase A for 30 min at room temperature in a light-protected area. The DNA content distribution was acquired in a FACSCalibur cytometer (Becton Dickinson), and it was analyzed using FlowJo software (Treestar, Inc.).

2.6. Cellular Morphology Analysis

The leukemia cells were treated with a vehicle or eribulin (0.25, 0.5, or 1 nM) for 72 h. For the morphology analysis, the vehicle- or eribulin-treated cells (1×10^5) were adhered to microscopic slides using cytospin (Serocito, Model 2400, FANEM, Guarulhos, Brazil) for the subsequent Rosenfeld staining. The morphological analyses of the nucleus and cytoplasm of the treated cells were visualized using a Leica DM 2500 optical microscope, and the images were acquired using the LAS V4.6 software (Leica, Benshein, Germany).

2.7. Colony Formation Assay

Colony formation was conducted in a semi-solid methylcellulose medium (0.5×10^3 cells/mL; MethoCult 4230; StemCell Technologies Inc., Vancouver, BC, Canada). The NB4, NB4-R2, MOLM3, OCI-AML3, Jurkat, and Namalwa cells were seeded in the presence of a vehicle or eribulin (0.12, 0.25, 0.5, or 1 nM) for eight days. The colonies were detected by adding 100 µL (5 mg/mL) of MTT reagent, and they were scored using the Image J quantification software (U.S. National Institutes of Health, Bethesda, MD, USA).

2.8. Western Blot Analysis

The cells were treated with a vehicle or eribulin (0.25, 0.5, and 1 nM) for 72 h, and the total protein was extracted using a buffer containing 100 mM Tris (pH 7.6), 1% Triton X-100, 2 mM PMSF, 10 mM Na_3VO_4, 100 mM NaF, 10 mM $Na_4P_2O_7$, and 4 mM EDTA. Equal amounts of protein (30 µg) were then subjected to SDS-PAGE, which was followed by electrotransfer to nitrocellulose membrane. The membranes were blocked with 5% milk, incubated with specific primary antibodies diluted in blocking buffer, and then, they were incubated with secondary antibodies conjugated to HRP (horseradish peroxidase). A Western blot analysis with the indicated primary antibodies was performed using the SuperSignal West Dura Extended Duration Substrate System (Thermo Fisher Scientific, San Jose, CA, USA) and a G: BOX Chemi XX6 gel document system (Syngene, Cam-

bridge, UK). The antibodies against stathmin 1 (OP18; sc-55531), p-stathmin 1^{S16} (p-OP18 Ser16; sc-12948-R), and γH2AX (sc-517348) were obtained from Santa Cruz Biotechnology (Santa Cruz, CA, USA). The antibodies against PARP1 (#9542) and α-tubulin (#2144) were from Cell Signaling Technology (Danvers, MA, USA). The band intensities were measured using the UN-SCAN-IT gel 6.1 software (Silk Scientific; Orem, UT, USA). The data were illustrated using multiple experiment viewer (MeV) 4.9.0 software [17]. The cropped gels retained the important bands, and the whole gel images are available in Figures S1 and S2.

2.9. Quantitative PCR (qPCR)

The total RNA was obtained using TRIzol reagent (Thermo Fisher Scientific). The cDNA was synthesized from 1 µg of RNA using a High-Capacity cDNA Reverse Transcription Kit (Thermo Fisher Scientific). Quantitative PCR (qPCR) was performed using a QuantStudio 3 Real-Time PCR System in conjunction with a SybrGreen System and specific primers (Table S1). *HPRT1* and *ACTB* were used as the reference genes. The relative quantification value was calculated using Equation $2^{-\Delta\Delta CT}$ [18]. A negative 'No Template Control' was included for each primer pair. The dissociation protocol was performed at the end of each run to check for non-specific amplification. The data were illustrated using MeV 4.9.0 software [17].

2.10. Statistical Analysis

The statistical analysis was performed using GraphPad Instat 5 (GraphPad Software, Inc.). An ANOVA test and a Bonferroni post-test were used for comparisons, and the Spearman test was used for the correlation analysis. All of the *p* values were two-sided with a significance level of 5%.

3. Results

3.1. Eribulin Reduces Cell Viability of Hematologic Neoplasm-Derived Cell Lines

Firstly, the antineoplastic activity of eribulin was evaluated in a large panel of myeloid and lymphoid cancer cell lines. Eribulin displays cytotoxic activity in the nanomolar range (IC_{50} values ranged from 0.13 to 12.12 nM), and only five out of twenty-one blood cancer cell lines were considered to be resistant to the drug (IC_{50} > 100 nM). Among the myeloid models, the cell lines with constitutive tyrosine kinase activation caused by the mutations BCR::ABL1 and $JAK2^{V617F}$ (K-562, KU812, SET-2, and HEL) presented higher IC_{50} values for eribulin (from 12.12 to >100 nM). Among the lymphoid models, the cell lines derived from multiple myeloma (U266, MM1.S, and MM1.R) presented higher IC_{50} values for eribulin (from 10.66 to 37.03 nM) (Figure 1A and Table S2). In the normal leukocytes, eribulin did not impact the cell viability, suggesting selectivity for malignant blood cells and a favorable therapeutic window (Figure 1A). Based on these findings, six acute leukemia cells were selected for a further analysis (NB4, NB4-R2, OCI-AML3, MOLM-13, Jurkat, and Namalwa). As shown in Figure 1B, eribulin exhibited dose- and time-dependent cytotoxicity in all of the leukemia cells assessed.

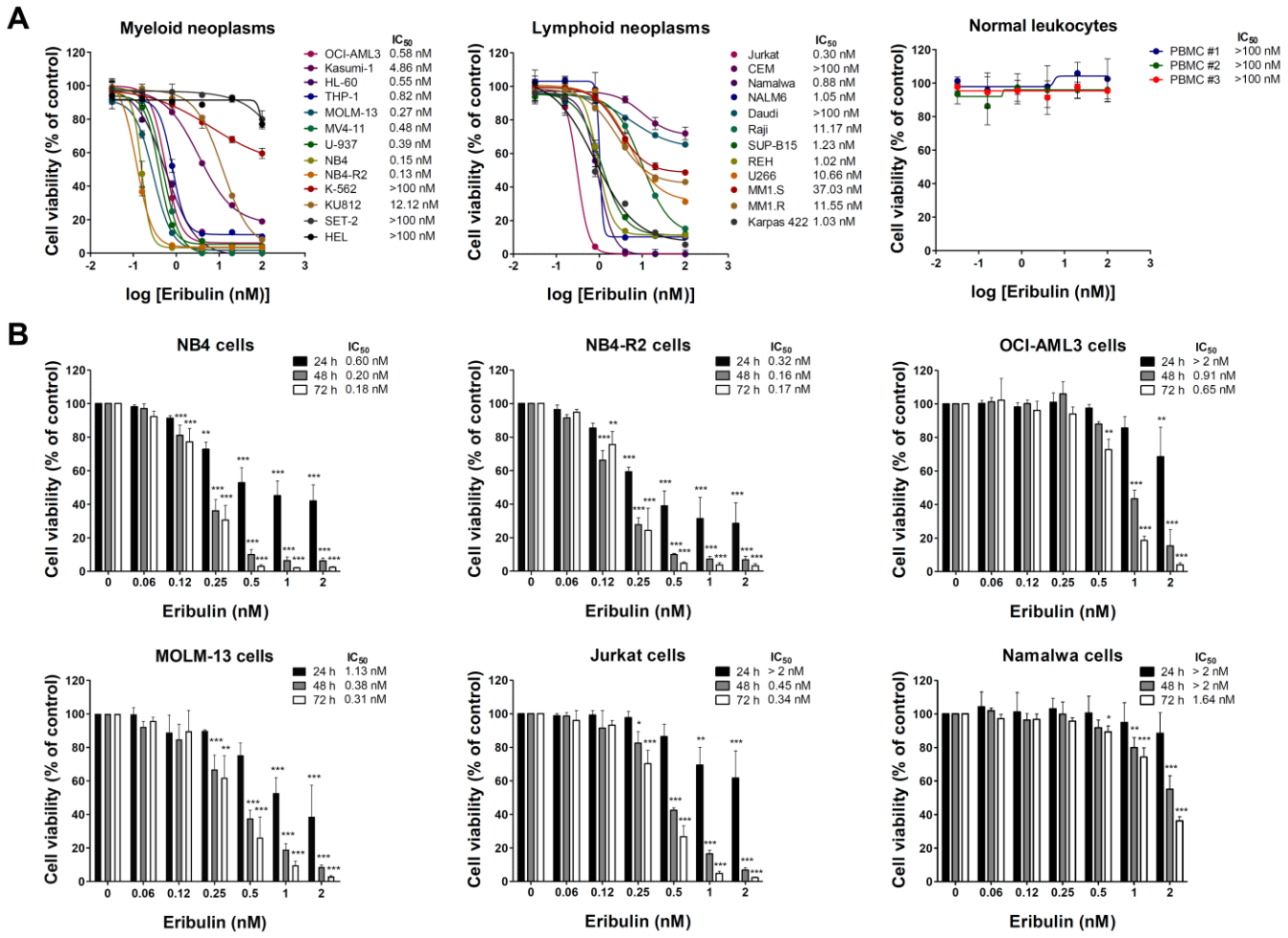

Figure 1. Eribulin exhibits selective dose- and time-dependent cytotoxic activity in blood cancer cells. (**A**) Dose–response curves were analyzed by methylthiazoletrazolium (MTT) assay in a panel of myeloid and lymphoid neoplasms cells or peripheral blood mononuclear cells (PBMC) from three healthy donors treated with increasing concentrations of eribulin (0.032–100 nM) for 72 h. We note that at the concentrations tested, the IC_{50} was not achieved (>100 nM) in normal leukocytes. (**B**) Bar graphs represent dose- and time-dependent responses to eribulin (0.06–2 nM) after 24, 48, and 72 h of exposure in NB4, NB4-R2, OCI-AML3, MOLM-13, Jurkat, and Namalwa cells. Values are expressed as the percentage of viable cells for each condition relative to untreated controls. Results are presented as mean ± SD of at least four independent experiments. The *p* values and cell lines are indicated in the graphs; * $p < 0.05$, ** $p < 0.01$, *** $p < 0.001$; ANOVA test and Bonferroni post-test.

3.2. Eribulin Promotes Apoptosis and Cell Cycle Arrest and Reduces Clonogenicity in Acute Leukemia Cells

Next, the cellular mechanisms triggered by eribulin in the leukemia cells were investigated. Eribulin significantly induced concentration-dependent apoptosis in the leukemia cells, as observed by phosphatidylserine exposure (all $p < 0.05$, Figure 2), and it increased the subG$_1$ cell populations (all $p < 0.05$, Figure 3). Eribulin also induced cell cycle arrest at the G$_2$/M phase for the NB4, NB-R2, OCI-AML3, and Jurkat cells and at the G$_0$/G$_1$ phase for MOLM-13 (all $p < 0.05$, Figure 3). The morphological analyses revealed a high frequency of mitotic aberrations upon conducting the treatment with eribulin for 72 h (Figure 4), which corroborates the cell cycle-related findings. Similarly, the long-term exposure to eribulin markedly decreased the autonomous clonal growth in the NB4, NB4-R2, MOLM-13, OCI-AML3, and Jurkat cells (all $p < 0.05$, Figure 5). The Namalwa cells were less sensitive to eribulin, which is consistent with the initial cell viability assays.

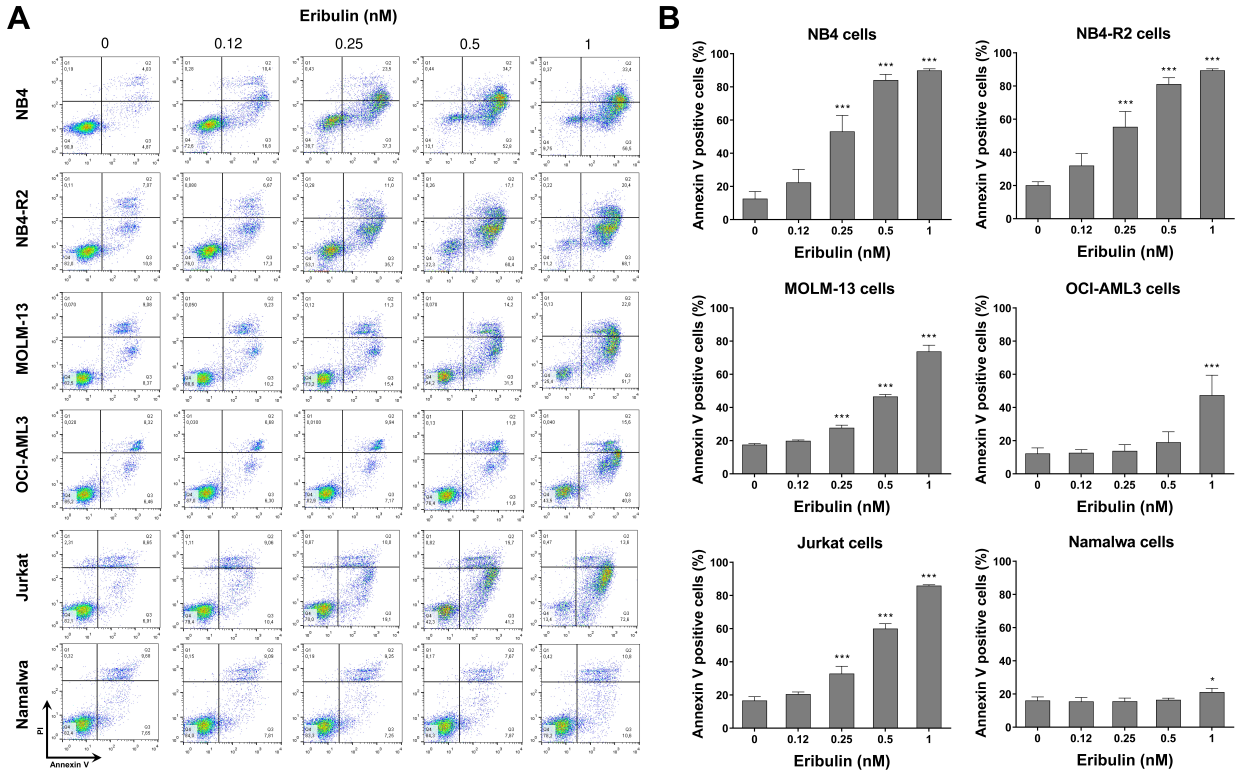

Figure 2. Eribulin triggers apoptosis in leukemia cells. (**A**) Apoptosis was detected by flow cytometry in NB4, NB4-R2, MOLM-13, OCI-AML3, Jurkat, and Namalwa cells treated with graded concentrations of eribulin (0.12, 0.25, 0.5, and 1 nM) for 72 h using the annexin V/propidium iodide staining method. Representative dot plots are shown for each condition; the upper and lower right quadrants (Q2 + Q3) cumulatively contain the apoptotic population (annexin V^+ cells). (**B**) Bar graphs represent the mean ± SD of at least four independent experiments quantifying apoptotic cell death. The *p* values and cell lines are indicated in the graphs; * $p < 0.05$, *** $p < 0.0001$; ANOVA test and Bonferroni post-test.

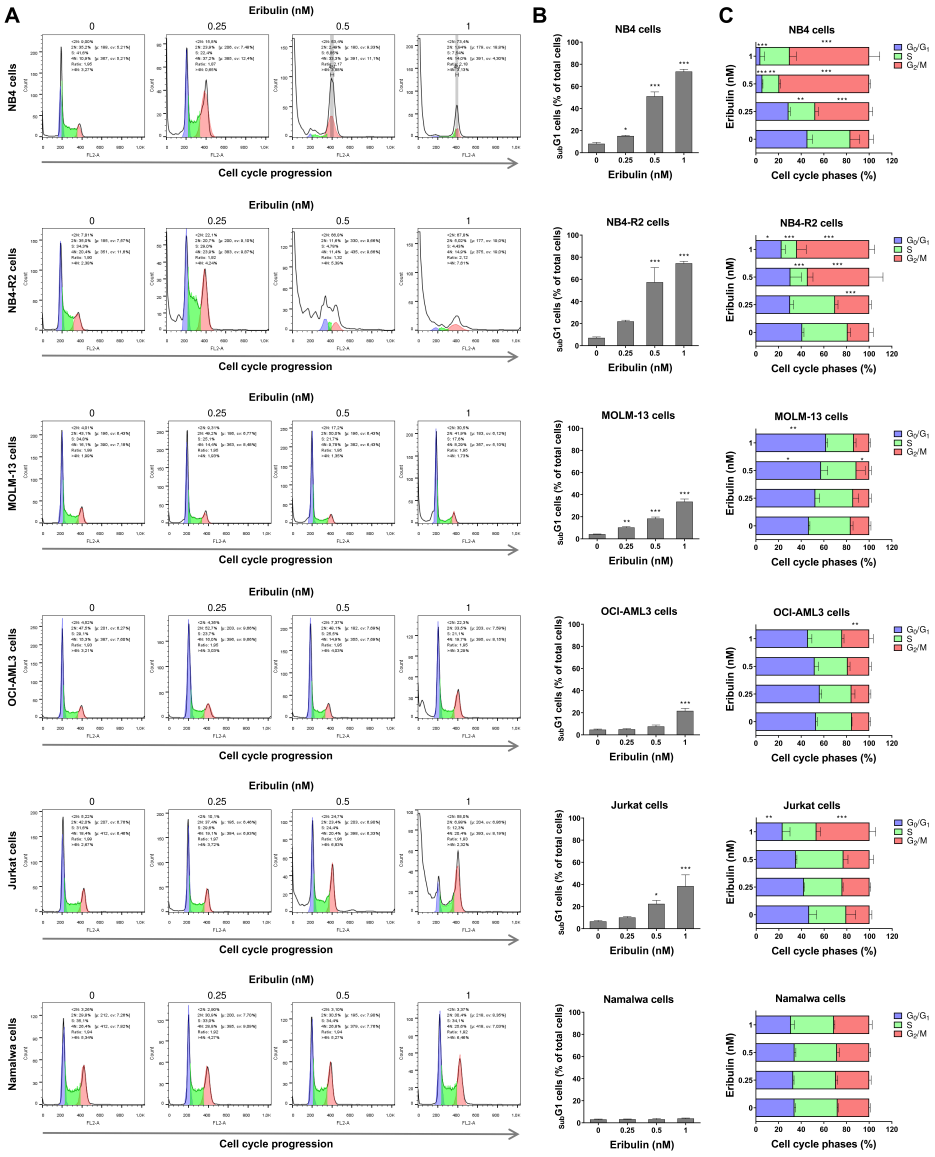

Figure 3. Eribulin arrests the cell cycle at G_2/M in leukemia cells. Cell cycle phases were determined by DNA content analysis by propidium iodide staining and flow cytometry in NB4, NB4-R2, MOLM-13, OCI-AML3, Jurkat, and Namalwa cells treated with eribulin (0.25, 0.5, and 1 nM) or vehicle for 72 h. (**A**) A representative histogram for each condition is presented. (**B**) The vertical bar graph represents the mean ± SD of the cell percentages in $subG_1$ from at least three independent experiments. (**C**) The horizontal bar graph represents the mean ± SD of cell distributions in the G_0/G_1, S, and G_2/M phases of the cell cycle (excluding $subG_1$) from at least three independent experiments. The *p* values and cell lines are indicated in the graphs; * $p < 0.05$, ** $p < 0.01$, *** $p < 0.001$; ANOVA and Bonferroni post-test.

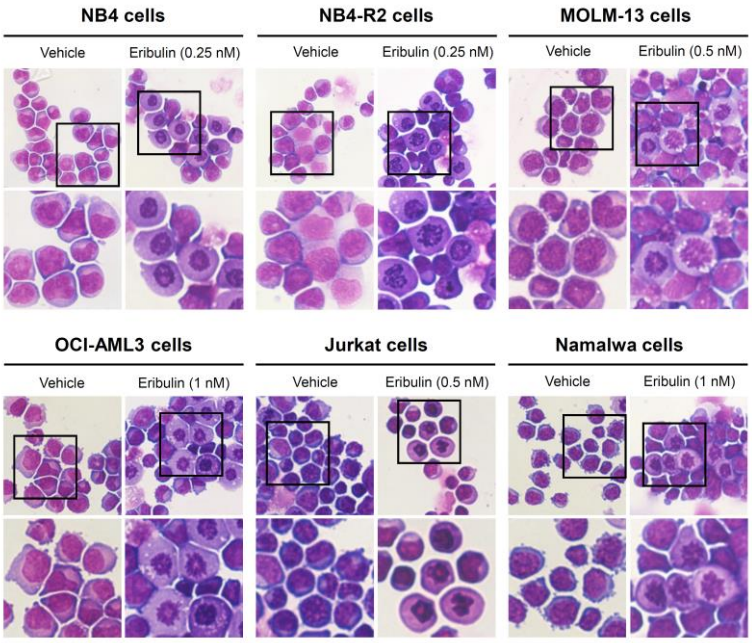

Figure 4. Aberrant mitoses are observed upon eribulin exposure in acute leukemia cells. NB4, NB4-R2, MOLM-13, OCI-AML3, Jurkat, and Namalwa cells were treated with vehicle or eribulin for 72 h, fixed, and stained with hematoxylin and eosin (H&E). The 400× and 1000× magnification images are displayed.

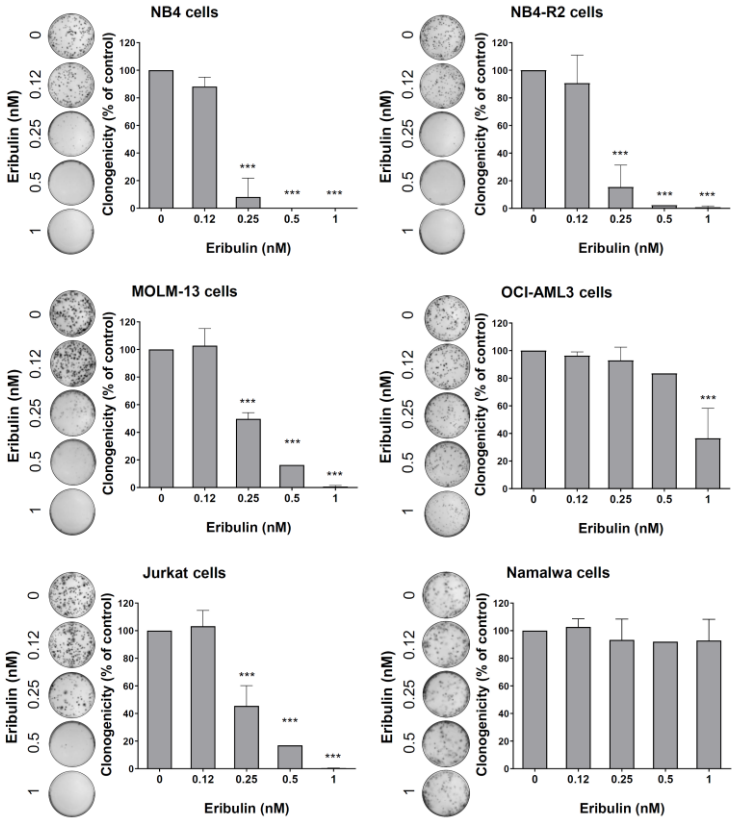

Figure 5. Eribulin reduces the clonogenicity of leukemia cells. Colonies containing viable cells were detected by adding an MTT reagent after eight days of culturing the cells in the presence of vehicle or eribulin (0.12, 0.25, 0.5, and 1 nM). Colony images are shown for one experiment, and bar graphs show the mean ± SD of at least three independent experiments. *** $p < 0.0001$; ANOVA test and Bonferroni post-test.